Development of the ICON dynamical core: modelling strategies and preliminary results

Luca Bonaventura

Max Planck Institut für Meteorologie
Hamburg, Germany
bonaventura@dkrz.de

ABSTRACT

An overview of the ICON project for the development of a nonhydrostatic GCM based on the icosahedral grid is presented. The main motivations, targets and features of the new model are outlined, with special attention to the expected improvements in simulating the stratosphere and the tropopause. The horizontal discretization approach is introduced, in the context of the shallow water model developed during the preliminary phase of the project. Numerical results obtained with the shallow water model are presented, showing that the proposed approach allows for accurate simulation of the main features of large scale atmospheric flows. The main open issues regarding the future model development are reviewed.

1 Outline of the ICON model development project

ICON (acronym for ICOsahedral Nonhydrostatic) is a joint project of the Max Planck Institute of Meteorology Hamburg (MPIfM) and the German Weather Forecasting Service (Deutscher Wetterdienst - DWD) for the development of a new general circulation model. The project target is a unified model for global and regional climate simulation and weather forecasting. The new model will be based on finite volume discretizations of the fully elastic, nonhydrostatic Navier-Stokes equations on geodesic, icosahedral, locally refinable grids. Various research institutes in Germany and elsewhere are also contributing to the project, among which PIK Potsdam, Freie Universität Berlin, AWI Bremerhaven, the Max Planck Institut for Computer Science in Saarbrücken and Colorado State University.

A number of reasons have lead to the choice of reshaping thoroughly the presently available models. Recent investigations (see e.g. [39]) have shown the problems arising when the spectral transform method is coupled to conservative, monotonic advection of tracers by finite volume schemes, among which some major inaccuracies in the simulation of troposphere - stratosphere tracer exchange. These problems are related to the lack of *consistency with the discrete continuity equation*, a concept whose relevance was already noticed in [1] and that has also been discussed in various recent studies on conservative advection schemes (see e.g. [30], [31]). It is easy to show that the discrepancy between the discretization of the divergence term in the continuity equation and in the tracer equations leads to an effective violation of mass conservation and monotonicity of tracer concentrations, even when flux form monotonic schemes are employed. Various idealized tests and a theorical analysis in the context of a simple shallow water model are reported in [21]. Possible fixes either do not solve the problem effectively or increase significantly the computational cost, if e.g. consistent velocity fields have to be computed on a finite difference grid by an *a posteriori* least squares fit. This problem cannot be reduced by simple means such as increasing the resolution and is a serious obstacle to accurate, conservative discretization of transport of chemical and moist species across the tropopause.

Another key issue is regionalization of climate and NWP models. All the nesting approaches currently implemented (at MPIfM, DWD or elsewhere) require strong smoothing at the boundaries of refined areas, because

of unappropriate treatment of the internal grid boundaries. The resulting models are not mass conservative and often display unphysical vertical velocities and precipitation patterns at the boundaries. Some approaches (conformal mappings, stretched lat-lon grids) allow to achieve locally higher resolutions, but their scope is limited to a small number of refined regions of special shape. Such approaches cannot be used for generalized grid refinement, e.g. over complex orographic features or over areas of special interest because of large tracer emissions. This contrasts with the great accuracy in the treatment of internal grid interfaces that has been achieved by fully conservative local grid refinement approaches developed over the last 20 years in the CFD community, along with efficient solvers to handle elliptic problems on locally refined grids and efficient dynamically adaptive algorithms (see e.g., among many others, [2], [4], [9], [10], [11], [17], [28], [30]). Although accurate models for geophysical flows that incorporate these features do not yet exist, their development appears rather attractive because of the potential gain in accuracy, efficiency and flexibility.

A relevant computational issue is also the fast growing cost of the Legendre transform computations required for higher resolution integrations of spectral models. Although great progress has been made in increasing the efficiency of such models, it would be desirable to consider for the next generation of climate and NWP GCMs discretization approaches that allow for the most efficient use of massively parallel computers.

From a more practical point of view, both MPIfM and DWD maintain up to now separate models for global and regional simulations, which entails unavoidable overhead and special interfaces for data exchange between the different models. The global and regional model of DWD are even using completely different grids and data structures and special interpolation operators are required to provide the boundary conditions to the regional model.

In order to find a practical solution that takes into account all these issues, MPIfM and DWD have started the ICON development project, which has begun its activity in May 2002. It is expected that close cooperation of MPIfM and DWD will also result into extensive testing of the new model in NWP mode and joint development of a new data assimilation system to be used by both institutions. Furthermore, the physical parameterization packages developed for ECHAM5, GME and LM will be incorporated in the new GCM. Full testing of the preliminary shallow water model is expected to be complete by the end of 2003 and a first operational version should be available by the end of 2005. The resulting model should replace the present global and regional models at MPIfM and DWD and constitute the atmospheric component of the Earth System Model under development at MPIfM.

The main features of the envisaged model formulation will be presented in sections 2 to 5. The expected advantages for modelling the stratosphere and the tropopause will be discussed in section 6. The horizontal discretization approach will be presented in section 7, in the context of a semi-implicit, mass conservative shallow water model that has been developed as a preliminary step towards the full three dimensional model. Numerical results obtained so far with this model are reported in section 8 and some of the main open issues regarding the future model development are discussed in section 9.

2 Model equations

The model under development in the ICON project will use the fully elastic, nonhydrostatic Navier-Stokes equations, which provide a framework that is sufficiently general for meteorological applications on most scales relevant for numerical weather prediction and climate simulation. In order to couple most consistently stratospheric and mesospheric chemical processes to the dynamics, air is considered as a multicomponent medium, consisting of

- a mixture of ideal gases (i.e., the constituents of *dry* air, which undergo chemical or photochemical reactions, but no phase change); the partial densities of these components will be denoted by $\rho_{d,k}$

- water vapour, which is also assumed to be an ideal gas, but which undergoes phase change; the partial density of this component will be denoted by ρ_v
- liquid water, which is assumed to be an incompressible fluid and the partial density of which will be denoted by ρ_l
- ice, which assumed to be and incompressible solid and the partial density of which will be denoted by ρ_f

The first assumption allows to consider the case in which the composition of dry air is changing, which is relevant for upper atmospheric applications. Denote the total density of air by

$$\rho = \sum_{k=1}^{N_d} \rho_{d,k} + \rho_v + \rho_l + \rho_f. \tag{1}$$

For meteorological applications, liquid water and ice contribute very little to the total specific volume and their contributions will be neglected in the derivation of an equation of state for air as a gas mixture. Furthermore, it is assumed that local thermodynamical equilibrium holds (so that a unique temperature can be defined for all gaseous constituents) and that the state equation of an ideal gas

$$p_k = R_k T \rho_k$$

holds for each gaseous constituent. Then, by Dalton's law

$$p = \Big[\sum_{k=1}^{N_d} R_{d,k} m_{d,k} + R_v m_v \Big] T \rho_d. \tag{2}$$

Here, p is the total air pressure, $\rho_d = \sum_{k=1}^{N_d} \rho_{k,d}$ is the total density of dry air, $R_{d,k}$ is the gas constant for the generic constituent of dry air, R_v is the gas constant for water vapour and m_k are the mixing ratios of the various species.

The precise formulation of the complete equations of motion for this multicomponent medium is still being discussed within the ICON project working groups, especially with respect to the description of the moist processes. A formulation of the basic dynamical equations of motion of dry air in the inviscid case which appears to have some advantages is the following:

$$\frac{\partial \rho_d}{\partial t} + \nabla \cdot (\rho_d \mathbf{v}) = 0 \tag{3}$$

$$\frac{\partial \mathbf{v}}{\partial t} = -\nabla K - (2\Omega + \zeta) \times \mathbf{v} - \frac{1}{\rho_d} \nabla \cdot p + \nabla \Phi + \mathbf{F}, \tag{4}$$

$$\frac{\partial (\rho_d \varepsilon)}{\partial t} + \nabla \cdot \Big[\Big(\rho_d \varepsilon + p + \mathbf{R} \Big) \cdot \mathbf{v} \Big] = 0 \tag{5}$$

Here, $\mathbf{v}$ denotes the velocity of dry air, which is interpreted as the baricentric velocity of the dry air components, thus allowing for a rigorous derivation of the energy balance (see e.g. [22]). ε is the total energy, K is kinetic energy, Ω denotes the rotation velocity of the Earth, $\zeta = \nabla \times \mathbf{v}$ is the relative vorticity, Φ denotes the normal gravity potential (see e.g. [54]), $\mathbf{F}$ denotes the resultant of the external forces (among which electromagnetic force plays an essential role above approximately 80 km height, where the presence of ionized particles begins to have a relevant impact on the neutral flow), $\mathbf{R}$ denotes the radiation heat flux. This set of equations has to be supplemented by conservation laws for the various (dry and moist) air components, chemical species and ions

$$\frac{\partial (\rho_d m_k)}{\partial t} + \nabla \cdot \Big[(\rho_d m_k) \mathbf{v} + \mathbf{J}_k^d \Big] = I_k. \tag{6}$$

Here, $\mathbf{J}_k^d$ denotes the diffusion flux with respect to the velocity of dry air, which needs to be approximated or parameterized, e.g. on the basis of Fick diffusion assumptions (see e.g. [25], [55]), whereas I_k denotes the sources or sinks of species k. This formulation would allow for application of efficient momentum advection schemes without spurious vorticity production (see e.g. [32]) and for total energy conservation. However, the formulation of the energy equation is currently being discussed further. Relevant issues for the final choice will be the concurrently designed treatment of the moist species, the desire to achieve an energy conserving formulation when also dissipative terms are included, the need for a formulation that is practical for semi-implicit time discretization. Results of the appropriate low Mach number asymptotics (see e.g. [29]) are also being taken into account.

3 The icosahedral grid

The basis for the spatial discretization developed in the ICON project will be the triangular grid obtained by recursive bisection of the regular icosahedron. The main reasons for this choice are its quasi-uniform coverage of the sphere, which solves automatically the pole problem and avoids artificially high Courant numbers, along with its hierarchical structure, that provides a very natural setting for local grid refinement. The use of such grids on the sphere goes back to the work of Arakawa, Sadourny and Williamson around 1968 [47], [56]. Their quasi-uniformity suggested that they could provide a viable alternative to latitude-longitude grids for high resolution simulations. Various finite difference and finite volume methods were developed on icosahedral grids (see [35], [57], [58]) for the barotropic vorticity equations and the shallow water equations, but also due to the development of models based on the spectral transform method, icosahedral discretizations were not pursued further in the 1970s (see e.g. the review of the earlier literature given in [59]). Two new developments took place in the 1980s, which somehow revived this line of research, along with the progressive improvement of the available hardware. On one hand, it was shown in [36] how the approach in [47] could be extended to the vorticity-divergence formulation of the shallow water equations, thus obtaining a numerical scheme that conserves energy and potential enstrophy. This inspired the further developments of [24], [52] and led to the development of general circulation models for climate applications within the BUGS project at CSU (see e.g. [44], [45]). On the other hand, Baumgardner introduced in [8] a sperical equivalent of linear finite elements based on the icosahedral grid. This led to the development of a semi-implicit scheme for the shallow water equations in [7], from which the primitive equation forecast model of DWD [33] has evolved. This model has been in operational use since December 1999 and is the only operational NWP model so far to be based on the icosahedral grid. Other finite element approaches based on geodesic grids have been introduced in [16], [20], [50].

In order to obtain numerical methods that are free of spurious pressure modes without recourse to large amounts of artificial diffusion, a staggered variable arrangement is envisaged. Staggered grid discretizations on the icosahedral grid have been proposed by Sadourny as early as [46], [48], although he did not investigate this approach further. S.Ničković analyzed the properties of C-type grid staggering in [37], [38]. Some of these analyses displayed the possibility of computational geostrophic modes for basic second order spatial discretization on plane, C-staggered hexagonal grids. On the other hand, efficient and accurate numerical schemes for realistic high resolution applications of the shallow water equations to estuarine dynamics have been developed in [13],[14]. In these papers, a C-grid variable arrangement was introduced on unstructured grids with the Voronoi-Delaunay property, which is shared by the icosahedral grids as well.

The grid construction process is the same as described in [8]. This construction yields a Delaunay triangulation of the sphere to which a Voronoi tessellation is naturally associated (see e.g. [3], [42]), which consists of convex spherical polygons (either pentagons or hexagons). The points of the icosahedral grid obtained in this way constitute the Voronoi grid on the sphere. Each of them belongs to a single hexagonal or pentagonal cell. The vertices of these polygons constitute the dual, or Delaunay grid, whose generic cell is defined as the convex

Level	N. of cells	N. of edges	Av. edge length (deg)	Av. edge length (km)
0	20	30	63.43	7053.89
1	80	140	33.86	3765.06
2	320	480	17.22	1914.39
3	1280	1920	8.64	961.26
4	5120	7680	4.33	481.14
5	20480	30720	2.17	220.43
6	81920	122880	1.08	120.32

Table 1: Features of the triangular icosahedral grids.

Level	A_{min}/A_{max}	$\lambda_{min}/\lambda_{max}$	Velocity point off-centering,%
0	1	1	0.0
1	0.83	0.88	19.9
2	0.89	0.80	12.0
3	0.92	0.78	6.5
4	0.93	0.78	3.4
5	0.94	0.78	1.7
6	0.94	0.78	0.97

Table 2: Quasi-uniformity of the triangular icosahedral grids after Heikes-Randall optimization.

hull of those Voronoi gridpoints whose cells have that vertex in common. The Delaunay cells of the icosahedral grid are all triangles. It can be proven (see e.g. the references in [26]) that for each side of a Voronoi cell there is a unique orthogonal side of the Delaunay cell associated to it. In this report, only results obtained using the (triangular) Delaunay cells as basic control volumes will be presented. The main features of the triangular icosahedral grid are shown in table 1. Some parameters highlighting its quasi-uniformity properties are displayed in table 2.

Let i denote the generic Delaunay cell and let l denote the generic edge of such a cell. Let $\mathscr{E}(i)$ denote the set of all edges of cell i and $\mathscr{C}(i)$ the set of all cells which have edges in common with cell i. The gridpoint associated to cell i will also be referred to as the cell center. The generic vertex of a cell, which is also the center of a cell in the dual grid, is denoted by v. $\mathscr{C}(v)$ denotes the set of all cells of which v is a vertex and $\mathscr{E}(v)$ denotes the set of all edges attached to vertex v. Let also $\mathbf{n}_l$ denote a unit vector normal to the edge l and let $\mathbf{t}_l$ denote the unit vector tangential to the edge l such that $\mathbf{n}_l \times \mathbf{k} = \mathbf{t}_l$. For each cell edge, an orientation $\sigma_{i,l}$ is defined so that $\sigma_{i,l}\mathbf{n}_l$ is the outer normal to the edge l of cell i. Given the edge l of a cell, the adjacent cells are denoted by the indexes $i(l,1)$ and $i(l,2)$, respectively. The indexes are chosen so that the direction from $i(l,1)$ to $i(l,2)$ is the positive direction of the normal vector $\mathbf{n}_l$. Vertex indexes $v(l,1)$ and $v(l,2)$ can also be defined analogously, so that the direction from $v(l,1)$ to $v(l,2)$ is the positive direction of the vector $\mathbf{t}_l$. The length of the edge l of a cell is denoted by λ_l and the distance between the centers of the cells adjacent to edge l (i.e., the length of a edge of the dual cell) is denoted by δ_l. The area of cell i is denoted by A_i.

For each cell edge, the *velocity points* of a C-type grid discretization are defined as the intersections between the edges of the Voronoi and Delaunay cells. By construction, each of these points is the midpoint of an edge of a Delaunay cell and equidistant from the centers of the adjacent Voronoi cells. A velocity point is also the intersection of the edge of the cell with the arc connecting the centers of the cells adjacent to that edge. These points are the locations of the discrete normal velocity components with respect to the cell edge. It should be observed that the velocity points are not equidistant from the adjacent Delaunay grid cell centers. However, grid optimization procedures such as those introduced in [23] can partly cure this problem, as shown in table 3, by reducing the off-centering to rather small values. Other optimization procedures, such as those of [53], do not guarantee that the optimized grid retains the Voronoi-Delaunay property. The C-type staggering on the

Delaunay grid is defined by specifying the discrete components of the velocity field normal to the cell edges at the velocity points and by specifying the discrete height (or pressure) values at the centers of the grid cells. It is to be remarked that this type of grid arrangement yields a spatial discretization which is very similar to what is obtained by the Raviart-Thomas elements of order 0 (see e.g. [40]). Furthermore, the discrete analogous of the Helmholtz decomposition theorem was proven in [41] for this type of grid arrangement.

4 Vertical discretization

The vertical discretization approach has only been outlined so far in a rather general way. Use of full spherical geometry is envisaged, without any simplification in the dependence of the metric coefficients on height. This entails abandoning also the so called traditional meteorological approximations and to make use of the *deep atmosphere* equations, see e.g. [51]. Regarding the vertical coordinate, due to the generality of the foreseen applications and to the needs of high resolution regional weather forecasting, a reasonable choice appears to be the use of a height based vertical coordinate, such as for example the hybrid terrain following coordinates that are common in mesoscale modelling. A height based coordinate would also be more practical for inclusion of the upper stratosphere and mesosphere in the same unified model framework. However, it is planned to take advantage as much as possible of formulations that are either coordinate invariant or that can be discretized without reference to a specific coordinate system, such as for example equations in flux form. Staggering of the vertical velocity component with respect to the pressure nodes in the vertical direction is also being considered.

5 Numerical methods

Finite volume techniques are being considered for the discretization of equations 3,5 and 6. This allows to achieve mass conservation in a straightforward way. Discontinous Galerkin techniques (see e.g. [15]) appear quite an attractive tool for the discretization of the tracer equations, since higher accuracy is achieved in a completely local way. This diminishes the need for communication among different processors if a domain decomposition parallelization is performed, which is of great importance for simulations with a large number of tracers, when tracer advection is responsible for a large share of the CPU time. Furthermore, these techniques are very flexible with respect to implementation on locally refined grids.

For the discretization of the momentum equation, finite difference schemes along the lines of [32] appear rather attractive, because they allow to combine the well known advantages of semi-lagrangian schemes with the absence of spurious vorticity production. It will be shown in section 7 how the Voronoi-Delaunay property of the icosahedral grid allows to extend the approach of [32] on quadrilateral lat-lon grids. However, it is also planned to implement an alternative semi-lagrangian option.

Semi-implicit time discretization appears a desirable target, in order to achieve optimal computational efficiency, provided that efficient solvers can be applied. This restricts somehow the range of possible spatial discretization approaches to those yielding relatively simple Helmholtz equations. Furthermore, as previously remarked, mass conservation and applicability on locally refined grids are essential *a priori* requirements for any approach considered viable for ICON. Again, an example of semi-implicit discretization is presented in section 7. A mass conservative extension to the full Euler equations could take place, for example, by application of a suitably modified version of the method introduced in [12]. Multigrid solvers (see e.g. [18], [49]) are quite naturally being considered as a basic tool for achieving optimal computational efficiency in the context of semi-implicit discretizations. Their potential for atmospheric modelling has already been shown in the past, see e.g. [5], [6], [24], [44]. Their applicability on locally refined grids has been shown for example in [4], [43]. Solvers based on the so called *cascadic multigrid* also display quite interesting properties, see e.g. [11], [10],

[28].

6 Expected advantages for stratospheric modelling

The first results obtained so far with the latest version of the MPIfM climate model (ECHAM5, soon to be released officially) seem to show that higher vertical resolution in the stratosphere does have a significant positive impact on the simulation of many tropospheric and stratospheric features. In validation runs that are being carried out on the AMIP test cases, the transport of water vapour across the tropopause and the downward control mechanisms appear to be simulated in a much more realistic way than in previous model versions (personal communication by E.Roeckner). Key stratospheric phenomena such as the quasi biennial oscillation have also been reproduced correctly in the ECHAM5 simulations with very high vertical resolution described in [19]. In order to achieve this, appropriate gravity wave parameterizations had to be employed, forcing a broad spectrum of atmospheric waves (see e.g. [34]). Furthermore, a vertical resolution varying between 0.7 and 1.0 km had to be used throughout the stratosphere. These capabilities of the ECHAM5 model will have to be preserved in the next step of the model evolution.

Regarding the ICON development project, the main specific target with respect to the modelling of the tropopause, stratosphere and mesosphere is the improved coupling of dynamical and photochemical processes. This should be achieved by allowing for a varying composition of dry air and by completely consistent discretization of the continuity equation and the flux form advection equations for the chemical species being considered. The inconsistency between the discrete formulation of the continuity equation and that of the mass fluxes in the tracer equations was shown in [39] to cause large errors for transport across the tropopause. The solutions proposed so far for this problem and evaluated in [39] do not seem to be effective. Therefore, it is expected that a model which is designed to be completely consistent with this respect leads to a significant improvement in mass conservative simulation of troposphere - stratosphere exchanges.

7 The shallow water model

A basic concept for the horizontal and semi-implicit time discretization of the the Euler equations will be presented here in the context of a numerical scheme for the shallow water equations. As customary for the development projects of global models, a prototype based on these simpler equations is being studied as a first step. Consider the vector invariant form of the shallow water equations on the sphere

$$\frac{\partial \mathbf{v}}{\partial t} = -(\zeta + f)\mathbf{k} \times \mathbf{v} - \nabla\Big(gh + K\Big), \tag{7}$$

$$\frac{\partial h}{\partial t} + \nabla \cdot \Big(h^* \mathbf{v}\Big) = 0, \tag{8}$$

where $\mathbf{v} = (u, v)$ is the horizontal velocity vector (on the sphere), $K = \frac{1}{2}(u^2 + v^2)$ is the kinetic energy, ζ is the vertical component of the relative vorticity, h^* is fluid depth, $h = h^* + h^s$ is the height of the free surface above mean sea level, h_s is the height of the orography, g is the gravitational constant and $\mathbf{k}$ the unit vector in the radial outward direction. In order to highlight the issue of consistency with the discrete continuity equation mentioned in section 1, also the conservation law for a passive tracer is considered,

$$\frac{\partial (qh)}{\partial t} + \nabla \cdot \Big(qh^* \mathbf{v}\Big) = 0, \tag{9}$$

where q denotes the tracer concentration.

Using the notation introduced in section 3, spatial discretization of the continuity equation (8) is straightforward by integration on cell i and application of the divergence theorem, so that one obtains

$$A_i \frac{\partial h_i}{\partial t} = - \sum_{l \in \mathscr{E}(i)} \sigma_{i,l} h_l^* u_l \lambda_l. \tag{10}$$

It is to be remarked that this approximation is by construction second order accurate on the triangular Delaunay grid. Although in principle an arbitrary discrete flux could be employed in the space discretization of the tracer conservation law (9), the resulting spatial discretization must be consistent with the spatial discretization of the continuity equation. This amounts to the statement that, given a tracer with unit discrete concentration values q_i, its discretized form must be identical to (10) (see e.g. [1]). This leads to a spatial discretization of the tracer conservation law (9) of the form

$$A_i \frac{\partial (q_i h_i)}{\partial t} = - \sum_{l \in \mathscr{E}(i)} \sigma_{i,l} q_l h_l^* u_l \lambda_l, \tag{11}$$

where the values q_l at the cell edges have to be reconstructed by means of appropriate interpolations. Specification if the interpolation procedure amounts to the choice of a specific advection scheme.

Taking the scalar product of equation (7) with the unit vector $\mathbf{n}_l$ at a generic velocity point yields, after use of the vector identity

$$(\mathbf{k} \times \mathbf{v}) \cdot \mathbf{n}_l = \mathbf{v} \cdot (\mathbf{n}_l \times \mathbf{k})$$

and of the definitions given in section 3, the equation

$$\frac{\partial u_l}{\partial t} = -(f_l + \zeta_l) v_l - \frac{\partial (gh + K)}{\partial \mathbf{n}_l}, \tag{12}$$

where v_l denotes the tangential velocity component $v_l = \mathbf{v} \cdot \mathbf{t}_l$. An analogous equation can be derived for the tangential velocity component. Thanks to the orthogonality between the cell edges and the arcs connecting the cell centers, the directional derivatives in the normal and tangential directions are easily approximated as

$$(\delta_v h)_l = \frac{h_{i(l,2)} - h_{i(l,1)}}{\delta_l} \qquad (\delta_\tau h)_l = \frac{h_{v(l,2)} - h_{v(l,1)}}{\lambda_l}.$$

It is to be remarked that the approximation of the derivative in the normal direction will be only first order accurate on the Delaunay grid, whose velocity points are not equidistant from the adjacent gridpoints. As noticed in section 3, grid optimization procedures such as those introduced in [23] can partially solve this problem. Furthermore, the normal velocity components are tangential to the edges of the dual cells, thus allowing to define the vertical component of vorticity on the dual Voronoi grid by Stokes theorem in a very natural way. It was shown in [41] that this definition of vorticity allows to prove a discrete equivalent of the Helmholtz decomposition theorem for the C type staggering described above. The values of ζ at the edge are then recovered by arithmetical mean. It is to be remarked that, computing the discrete circulation of equation 12, a spatially discretized equation for the evolution of ζ is obtained.

A semi-implicit time discretization of equations (7)-(8) will be considered, in order to improve efficiency for high resolution simulations. For simplicity, only a simple two time level scheme based on the trapezoidal integration rule is considered here, that is given by

$$u_l^{n+1} = u_l^n - \Delta t (f_l + \tilde{\zeta}_l^{n+\alpha}) v_l^{n+\alpha} - \Delta t \left[\delta_v (g h^{n+\alpha} + \tilde{K}^{n+\alpha}) \right]_l \tag{13}$$

$$A_i h_i^{n+1} = A_i h_i^n - \Delta t \sum_{l \in \mathscr{E}(i)} \sigma_{i,l} h_l^* u_l^{n+\alpha} \lambda_l. \tag{14}$$

Here, $\phi^{n+\alpha} = \alpha\phi^{n+1} + (1-\alpha)\phi^n$, $h_l^* = h_l^n - h_l^s$ and $\alpha \in [\frac{1}{2}, 1]$ for stability, with $\alpha = \frac{1}{2}$ yielding a second order accurate time discretization in the linear case. On the other hand, $\tilde{\psi}^{n+\alpha}$ denotes some estimate of the value of ψ at time $(n+\alpha)\Delta t$ obtained by an explicit discretization. Along the lines of [32], where a more advanced flux form semi-lagrangian scheme was applied in an analogous step, a simple upwind discretization is employed in this preliminary implementation for these intermediate updates. Since the discrete values of ζ are naturally defined at the vertices of the triangular cells, the intermediate update of ζ is computed by a discretization using as control volumes the dual hexagonal/pentagonal cells.

The value of the tangential velocity component at timestep $n+1$ can be recovered by deriving the analogous of equation 12 for the tangential velocity component and performing again a semi-implicit time discretization. This yields

$$v_l^{n+1} = v_l^n + \Delta t(f_l + \tilde{\zeta}_l^{n+\alpha})u_l^{n+\alpha} - \Delta t\left[\delta_\tau(gh^{n+\alpha} + \tilde{K}^{n+\alpha})\right]_l. \tag{15}$$

Here, the values v_l^n are to be determined by reconstruction of the full velocity vector at time n at the velocity node l. In this implementation, standard linear reconstruction from Raviart-Thomas finite element theory (see e.g. [40]) was employed to obtain a velocity vector at the mass points, whose components were then averaged onto the cell edge. Other simpler reconstruction approaches are discussed in [41]. Furthermore, in order to compute $\delta_\tau(gh^{n+\alpha} + \tilde{K}^{n+\alpha})$ values of $h^{n+\alpha}, \tilde{K}^{n+\alpha}$ at the vertices of the triangular cells have to be computed. In the present preliminary implementation, this is done by simple area weighted averaging.

Substituting equation (15) into (13) yields

$$\begin{aligned} u_l^{n+1} \quad &= \gamma_l \mathscr{F}_l^n(u) \\ &+ g\gamma_l(f_l + \tilde{\zeta}_l^{n+\alpha})\alpha^2\Delta t^2(\delta_\tau h^{n+1})_l - g\gamma_l\alpha\Delta t(\delta_v h^{n+1})_l \end{aligned} \tag{16}$$

where

$$\begin{aligned} \mathscr{F}_l^n(u) \quad &= u_l^n - \Delta t(f_l + \tilde{\zeta}_l^{n+\alpha})v_l^n - \alpha(1-\alpha)\Delta t^2(f_l + \tilde{\zeta}_l^{n+\alpha})^2 u_l^n \\ &+ \alpha(1-\alpha)\Delta t^2 g(f_l + \tilde{\zeta}_l^{n+\alpha})(\delta_\tau h^n)_l - g(1-\alpha)\Delta t(\delta_v h^n)_l \end{aligned}$$

and $\gamma_l = 1/(1 + \alpha^2\Delta t^2(f_l + \tilde{\zeta}_l^{n+\alpha})^2)$. Substitution of (16) into (14) yields for each cell i the discrete wave equation

$$\begin{aligned} A_i h_i^{n+1} \quad &- g\alpha^2\Delta t^2 \sum_{l \in \mathscr{E}(i)} \left[(\delta_v h^{n+1})_l - \alpha\Delta t(f_l + \tilde{\zeta}_l^{n+\alpha})(\delta_\tau h^{n+1})_l\right] \gamma_l \sigma_{i,l} h_l^* \lambda_l \\ &= \mathscr{F}_i^n(h), \end{aligned} \tag{17}$$

where

$$\begin{aligned} \mathscr{F}_i^n(h) = A_i h_i^n \quad &- (1-\alpha)\Delta t \sum_{l \in \mathscr{E}(i)} \sigma_{i,l} h_l^* u_l^n \lambda_l \\ &- \alpha\Delta t \sum_{l \in \mathscr{E}(i)} \sigma_{i,l} h_l^* \gamma_l \mathscr{F}_l^n(u) \lambda_l. \end{aligned}$$

The set of all equations (17) for each cell i yields a linear system in the unknowns h_i^{n+1}. Its matrix is sparse and its symmetric part is positive definite and diagonally dominant. Furthermore, the asymmetric part of the matrix

is multiplied by the Coriolis coefficient, so that the resulting matrix is actually a relatively weak asymmetric perturbation of an M-matrix. In the present implementation, its solution is computed by fixed point iterations in which the preconditioned conjugate gradient method is used in each iteration for the symmetric part.

Finally, since time discretization of (10) and (11) must also preserve consistency with continuity, as remarked in [21], the conservation law for the tracer should be discretized in time accordingly as

$$q_i^{n+1} h_i^{n+1} = q_i^n h_i^n - \frac{\Delta t}{A_i} \sum_{l \in \mathscr{E}(i)} \sigma_{i,l} q_l h_l^* u_l^{n+\alpha} \lambda_l. \tag{18}$$

8 Numerical results

A number of numerical tests is being carried out in order to assess the effective accuracy of the discretization outlined above. The tests have been performed with a preliminary implementation of the method described in section 7. In this implementation, for simplicity, the nonlinear terms were dropped in equation15. Furthermore, simple interpolation and vector reconstruction approaches were employed, as previously mentioned. Complete quantitative evaluation of the performance of an improved implementation on the basis of the standard shallow water test suite in [60] is currently under way. Here, only a few selected and preliminary results will be reported.

Firstly, due to concerns about the capability of C grid staggered arrangements to describe properly geostrophic equilibrium (see e.g. [38]), a test case is considered for the linear shallow water equations. The fluid is initially at rest and the height field is initialized with the initial datum shown in figure1, in which a zonally symmetric perturbation of about $500m$ was superimposed to a constant height field $h_0 = 2000m$. Geostrophic adjustment of the initially unbalanced state generates a fast propagating gravity wave, shown in figures2,3 at times $t = 24h$ and $t = 48h$, respectively, along with the balanced height field close to the pole. The simulation was performed at various resolutions with analogous results, those shown here are for a grid size of approximately $220km$ and a gravity wave Courant number 1.5 approximately. The gravity wave propagates at approximately the correct speed, altough with the expected phase delay due to the semi-implicit discretization.

Test cases 5 and 6 of the standard shallow water test suite in [60] have also been run. The height field for test 5 (flow over an isolated mountain) is shown at day 10 in figure4, as computed with a grid size of approximately $120km$ and a gravity wave Courant number 1.5 approximately. The height field for test case 6 (Rossby Haurwitz wave) at day 7 is shown in figure 5, as computed with a grid size of $240km$ approximately and a gravity wave Courant number 1.5 approximately. Figures 4,5 can be compared directly with figures 5.1c, 5.5c of [27], respectively (the same contours have been used for each plot as in those figures). Good quantitative agreement with the reference spectral solution is displayed. Analogous results have been obtained also at coarser resolutions, although longer term integrations gave so far larger errors with respect to the reference solutions.

9 Open issues and development plans

Although the preliminary results of the proposed horizontal and time discretization approach appear promising, a more accurate implementation must be achieved and a number of important features of the future ICON model have yet to be fully specified. A choice has to be made on the formulation of the energy equation and on the representation of the moist processes The precise formulation of the 3D model equations and a unified design of the parameterization packages should be achieved within 2003. Applications to realistic stratospheric modelling are still a long way ahead, but idealized stratospheric tests could be run within the next few months.

Acknowledgements

This work has been carried out at MPIfM during my leave of absence from the University of Trento, Italy. I would like to thank Erich Roeckner and all the other members of the ECHAM5 team at MPIfM Hamburg for their great help and support. I also would like to thank Detlev Majewski of DWD for many discussions on numerical models on icosahedral grids and for having warmly sponsored the ICON project from the very start. Intensive discussions with all the ICON WG1 members are gratefully acknowledged and special thanks go to Nicola Botta, Marco Giorgetta, Rupert Klein and Todd Ringler for continuous and fruitful exchange of ideas. The icosahedral grid generator employed has been developed from a code that was kindly made available by John Thuburn.

References

[1] A.Arakawa and V.Lamb. A potential enstrophy and energy conserving scheme for the shallow water equations. *Monthly Weather Review*, 109:18–136, 1981.

[2] A. S. Almgren, J.B. Bell, P. Colella, L.Howell, and M.L. Welcome. A conservative adaptive projection method for the variable density incompressible Navier-Stokes equations. *Journal of Computational Physics*, 142:1–46, 1998.

[3] J.M. Augenbaum and C.S. Peskin. On the construction of the Voronoi mesh on the sphere. *Journal of Computational Physics*, 59:177–192, 1985.

[4] D. Bai and A. Brandt. Local mesh refinement multilevel techniques. *SIAM Journal of Scientific Computing*, 8:109–134, 1987.

[5] S.R.M. Barros, D.P. Dee, and F. Dickstein. A multigrid solver for semi-implicit global shallow-water models. *Atmosphere-Ocean*, 28:24–47, 1990.

[6] J.R. Bates, F.H.M. Semazzi, R.W. Higgins, and S.R.M. Barros. Integration of the shallow water equations on the sphere using a vector semi-lagrangian scheme with a multigrid solver. *Monthly Weather Review*, 118:1615–1627, 1990.

[7] John R. Baumgardner. A semi-implicit semi-lagrange method for the shallow water equations on a triangular mesh. In *Proceedings of the 4th CHAMMP Workshop for the Numerical Solution of PDEs in Spherical Geometry*, page 1. Department of Energy, USA, 1994.

[8] John R. Baumgardner and Paul O. Frederickson. Icosahedral discretization of the two-sphere. *SIAM Journal of Scientific Computing*, 22(6):1107–1115, December 1985.

[9] M. J. Berger and P. Colella. Local adaptive grid refinement for shock hydrodynamics. *Journal of Computational Physics*, 82:64–84, 1989.

[10] L. Bonaventura and G. Rosatti. A cascadic conjugate gradient algorithm for mass conservative, semi-implicit discretization of the shallow water equations on locally refined structured grids. *International Journal of Numerical Methods in Fluids*, 40:217–230, 2002.

[11] F.A. Bornemann and P. Deuflhard. The cascadic multigrid method for elliptic problems. *Numerische Mathematik*, 75:135–152, 1996.

[12] V. Casulli and D. Greenspan. Pressure method for the numerical solution of transient, compressible fluid flows. *International Journal of Numerical Methods in Fluids*, 4:1001–1012, 1984.

[13] V. Casulli and R.A. Walters. An unstructured grid, three-dimensional model based on the shallow water equations. *International Journal of Numerical Methods in Fluids*, 32:331–348, 2000.

[14] V. Casulli and P. Zanolli. A three-dimensional semi-implicit algorithm for environmental flows on unstructured grids. In *Proceedings of Numerical Methods for Fluid Dynamics VI, Oxford, UK*, pages 57–70. M. J. Baines Ed., ICFD Oxford University Computing Laboratory, 1998.

[15] B. Cockburn and C.W. Shu. The Runge-Kutta Discontinuous Galerkin method for conservation laws, V. *Journal of Computational Physics*, 141:198–224, 1998.

[16] M.J.P. Cullen. Integration of the primitive barotropic equations on a sphere using the finite element method. *Quarterly Journal of the Royal Meteorological Society*, 100:555, 1974.

[17] M.G. Edwards. Elimination of adaptive grid interface errors in the discrete cell centered pressure equation. *Journal of Computational Physics*, 126:356–372, 1996.

[18] Scott R. Fulton, Paul E. Ciesielski, and Wayne H. Schubert. Multigrid methods for elliptic problems: A review. *Monthly Weather Review*, 114:943–959, May 1986.

[19] M. A. Giorgetta, E. Manzini, and E. Roeckner. Forcing the quasi-biennial oscillation from a broad spectrum of atmospheric waves. *Geophysical Research Letters*, 29:86–1:4, 2002.

[20] Francis X. Giraldo. Lagrange-Galerkin methods on spherical geodesic grids: The shallow water equations. *Journal of Computational Physics*, 160:336–368, 2000.

[21] E.S. Gross, L. Bonaventura, and G. Rosatti. Consistency with continuity in conservative advection schemes for free-surface models. *International Journal of Numerical Methods in Fluids*, 38:307–327, 2002.

[22] I. Gyarmati. *Non-equilibrium Thermodynamics*. Springer Verlag, 1970.

[23] Ross Heikes and David A. Randall. Numerical integration of the shallow-water equations on a twisted icosahedral grid. Part II: A detailed description of the grid and an analysis of numerical accuracy. *Monthly Weather Review*, 123:1881–1887, June 1995.

[24] Ross Heikes and David R. Randall. Numerical integration of the shallow-water equations on a twisted icosahedral grid. Part I: Basic design and results of tests. *Monthly Weather Review*, 123:1862–1880, June 1995.

[25] F. Herbert. Prigogine's diffusion theorem and its application to atmospheric transfer processes: Part 2, invariance properties and Fick type diffusion laws. *Contributions to Atmospheric Physics*, 56:480–494, 1983.

[26] F. Hermeline. Two coupled particle-finite volume methods using Delaunay-Voronoi meshes for the approximation of Vlasov-Poisson and Vlasov-Maxwell equations. *Journal of Computational Physics*, 106:1–18, 1993.

[27] Ruediger Jakob-Chien, James J. Hack, and David L. Williamson. Spectral transform solutions to the shallow water test set. *Journal of Computational Physics*, 119:164–187, 1995.

[28] K.Lackner and R.Menikoff. Multiscale linear solvers for very large systems derived from PDE. *SIAM Journal of Scientific Computing*, 21:1950–1968, 2000.

[29] R. Klein. Asymptotic analyses for atmospheric flows and the construction of asymptotically adaptive numerical methods. *Z. für Angewandte Mathematik und Mechanik*, 80:765–777, 2000.

[30] Randall J. Leveque. High-resolution conservative algorithms for advection in incompressible flow. *SIAM Journal of Scientific Computing*, 33(2):627–665, April 1996.

[31] Shian-Jiann Lin and Richard B. Rood. Multidimensional flux-form semi-Lagrangian transport schemes. *Monthly Weather Review*, 124:2046–2070, September 1996.

[32] Shian-Jiann Lin and Richard B. Rood. An explicit flux-form semi-Lagrangian shallow water model on the sphere. *Quarterly Journal of the Royal Meteorological Society*, 123:2477–2498, 1997.

[33] Detlev Majewski, Dörte Liermann, Peter Prohl, Bodo Ritter, Michael Buchhold, Thomas Hanisch, Gerhard Paul, Werner Wergen, and John Baumgardner. The operational global icosahedral-hexagonal gridpoint model GME: description and high resolution tests. *Monthly Weather Review*, 130:319–338, 2002.

[34] E. Manzini, N.A. McFarlane, and C. McLandress. Impact of the Doppler spread parameterization on the simulation of the middle atmosphere. *Journal of Geophysical Research*, 102:25751–25762, 1997.

[35] Y. Masuda. A finite difference scheme by making use of hexagonal mesh-points. In *Proceedings of the WMO/IUGG NWP Symposium, Tokyo*, pages 35–45. Japan Meteorological Agency, 1969.

[36] Y. Masuda and H. Ohnishi. An integration scheme of the primitive equation model with a icosahedral-hexagonal grid system and its application to the shallow water equations. In *Proceedings of the WMO/IUGG NWP Symposium, Tokyo*, page 317. Japan Meteorological Agency, 1986.

[37] S. Ničković. On the use of hexagonal grids for simulation of atmospheric processes. *Contributions to Atmospheric Physics*, 67(2):103–107, May 1994.

[38] S. Ničković, M.B.Gavrilov, and I.A. Tošić. Geostrophic adjustment on hexagonal grids. *Monthly Weather Review*, 130(3):668–683, 2002.

[39] P.Jöckel, R. von Kuhlmann, M.G. Lawrence, B.Steil, C.A.M. Brenninkmeijer, P.J. Crutzen, P.J. Rasch, and B.Eaton. On a fundamental problem in implementing flux-form advection schemes for tracer transport in 3-dimensional general circulation and chemistry transport models. *Quarterly Journal of the Royal Meteorological Society*, 127:1035–1052, 2001.

[40] Alfio Quarteroni and Alberto Valli. *Numerical approximation of partial differential equations*, chapter 9: The Stokes problem. Springer Verlag, 1994.

[41] R.A.Nicolaides. Direct discretization of planar div-curl problems. *SIAM Journal of Numerical Analysis*, 29:32–56, 1992.

[42] S. Rebay. Efficient unstructured mesh generation by means of Delaunay triangulation and Bowyer-Watson algorithm. *Journal of Computational Physics*, 106:125–138, 1993.

[43] R.Hess. Dynamically adaptive multigrid on parallel computers for a semi-implicit discretization of the shallow water equations. Technical Report 1999/9, GMD, 1999.

[44] Todd D. Ringler, Ross P. Heikes, and David A. Randall. Modeling the atmospheric general circulation using a spherical geodesic grid: A new class of dynamical cores. *Monthly Weather Review*, 128:2471–2490, July 2000.

[45] Todd D. Ringler and David A. Randall. A potential enstrophy and energy conserving numerical scheme for solution of the shallow-water equations a geodesic grid. *Monthly Weather Review*, 130:1397–1410, July 2002.

[46] R. Sadourny. Numerical integration of the primitive equations on a spherical grid with hexagonal cells. In *Proceedings of the WMO/IUGG NWP Symposium, Tokyo*, pages 45–52. Japan Meteorological Agency, 1969.

[47] R. Sadourny, A. Arakawa, and Y.Mintz. Integration of the nondivergent barotropic vorticity equation with a icosahedral-hexagonal grid for the sphere. *Monthly Weather Review*, 96:351–356, August 1968.

[48] R. Sadourny and P.Morel. A finite difference approximation of the primitive equationsfor a hexagonal grid on a plane. *Monthly Weather Review*, 97:439–445, 1969.

[49] K. Stüben and U. Trottenberg. Multigrid methods: fundamental algorithms, model problem analysis and applications. In *Lecture Notes in Mathematics, 960*. Springer Verlag, 1992.

[50] G. R. Stuhne and W. R. Peltier. New icosahedral grid-point discretizations of the shallow water equations on the sphere. *Journal of Computational Physics*, 148:23–58, 1999.

[51] J. Thuburn, N.Wood, and A. Staniforth. Normal modes of deep atmospheres, I: spherical geometry. *Monthly Weather Review*, 128:1771–1792, 2002.

[52] John Thuburn. A PV-based shallow-water model on a hexagonal-icosahedral grid. *Monthly Weather Review*, 125:2328–2347, September 1997.

[53] H. Tomita, M. Tsugawa, M.Satoh, and K.Goto. Shallow water model on a modified icosahedral grid by using spring dynamics. *Journal of Computational Physics*, 174:579–613, 2001.

[54] W. Torge. *Geodesy.* W. de Gruyter, 2001.

[55] U. Wacker and F. Herbert. Continuity equations as expressions for local balances of masses in cloudy air. *Tellus A*, to appear, 2003.

[56] David L. Williamson. Integration of the barotropic vorticity equation on a spherical geodesic grid. *Tellus*, 20:642–653, 1968.

[57] David L. Williamson. Numerical integration of fluid flow over triangular grids. *Monthly Weather Review*, 97:885–895, 1969.

[58] David L. Williamson. Integration of the primitive barotropic model over a spherical geodesic grid. *Monthly Weather Review*, 98:885–895, 1970.

[59] David L. Williamson. *Numerical methods used in atmospheric models, Volume II*, chapter 2: Difference approximations for fluid flow on a sphere., pages 53–123. WMO, GARP Publication series n.17, 1979.

[60] David L. Williamson, John B. Drake, James J. Hack, Rüdiger Jakob, and Raul N. Swarztrauber. A standard test set for numerical approximations to the shallow water equations in spherical geometry. *Journal of Computational Physics*, 102:221–224, 1992.

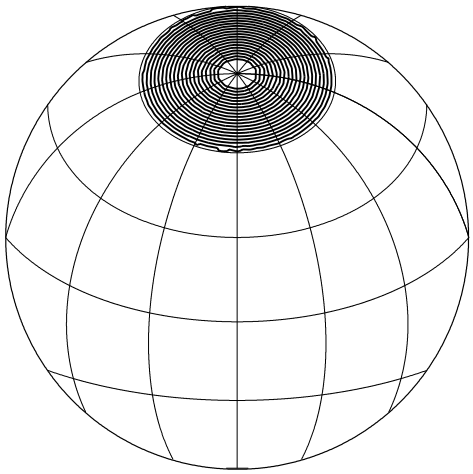

Figure 1: Initial height field for geostrophic adjustment test case, contours every 20 m.

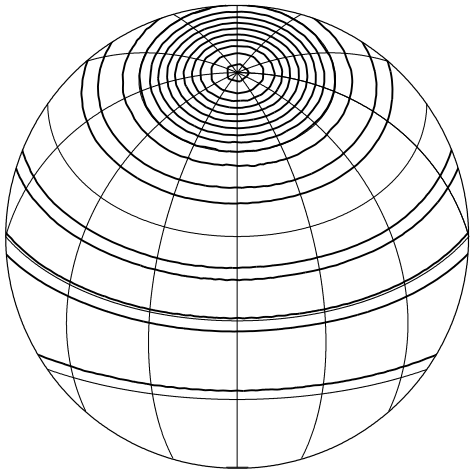

Figure 2: Height field at day 1 for geostrophic adjustment test case

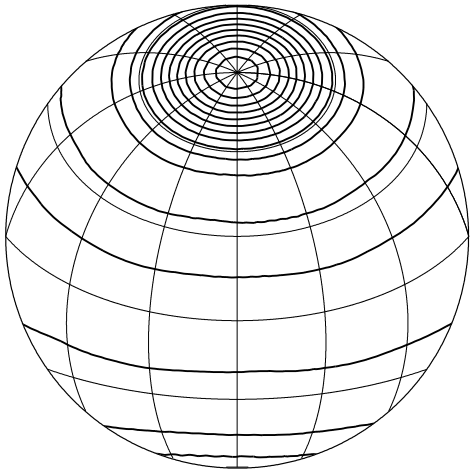

Figure 3: Height field at day 2 for geostrophic adjustment test case

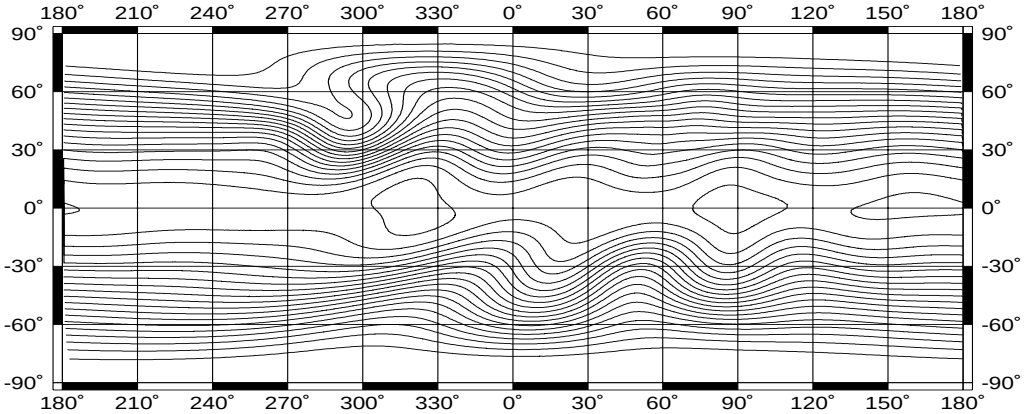

Figure 4: Height field at day 10 for test case 5

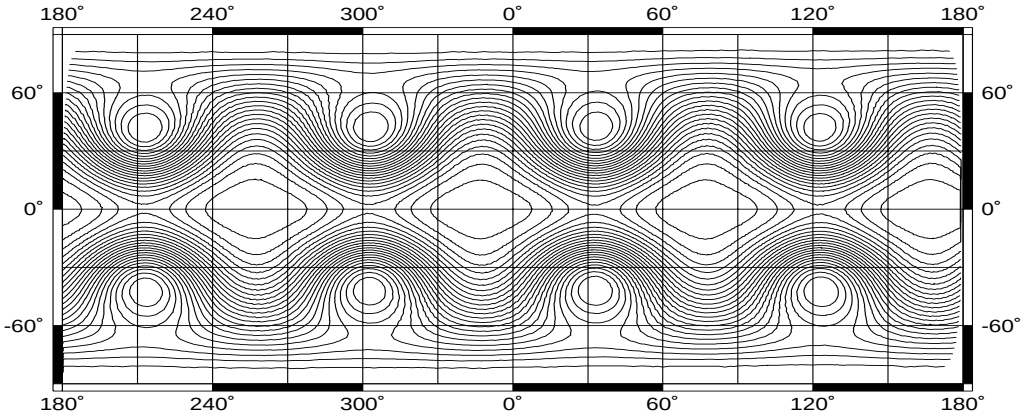

Figure 5: Height field at day 7 for test case 6